Experimental and simulated solute transport in a partially-saturated, variable-aperture fracture

Russell L. Detwiler[1] and Harihar Rajaram

Department of Civil, Environmental, and Architectural Engineering, University of Colorado, Boulder, USA

Robert J. Glass

Flow Visualization and Processes Laboratory, Sandia National Laboratories, Albuquerque, New Mexico, USA

Received 22 May 2001; revised 7 August 2001; accepted 6 September 2001; published 30 April 2002.

[1] We compare solute transport experiments to simulations in a partially-saturated, variable-aperture fracture in measured fracture aperture and entrapped-air geometry fields. The computational model tracks particles through a quasi-three-dimensional velocity field that is based on the two-dimensional solution to the Reynolds equation. The model predicts 84% of the relative increase in dispersion caused by the entrapped phase, and reproduces the experimentally observed nonlinear velocity-dependence of solute dispersion. *INDEX TERMS:* 1832 Hydrology: Groundwater transport; 1829 Hydrology: Groundwater hydrology

1. Introduction

[2] For a saturated fracture in an impermeable matrix, solute dispersion is controlled by velocity variations that result from a combination of the velocity profile across the fracture aperture (Taylor dispersion) and aperture variability over the fracture-plane (macrodispersion). This combined influence has been studied in saturated fractures [*Ippolito et al.*, 1994; *Roux et al.*, 1998; *Detwiler et al.*, 2000] and results in a nonlinear *Pe*-dependence of fracture-scale estimates of the longitudinal dispersion coefficient (D_L), where the Peclet number, $Pe = \hat{V}\hat{b}/D_m$, $\hat{V}$ is the mean solute velocity, $\hat{b}$ is the mean aperture, and D_m is the molecular diffusion coefficient. Introducing a nonwetting, immiscible phase, such as air or nonaqueous-phase liquid (NAPL), into a variable-aperture fracture will result in entrapped regions with spatial distribution controlled by aperture variability within the fracture and the combined influences of capillary, gravitational, and viscous forces during invasion of the nonwetting fluid [*Glass et al.*, 1995]. Entrapped regions will enhance flow channeling and thus increase in-plane velocity variations and solute dispersion in the fracture. The influence of entrapped-air geometry on solute transport in variable aperture fractures has been studied qualitatively [*Glass and Nicholl*, 1995], but we are unaware of quantitative investigations in partially-saturated fractures.

[3] Our objectives are, first, to evaluate our ability to simulate transport in a partially-saturated fracture and, second, to investigate the relative influence of in-plane and out-of-plane velocity variability on solute dispersion in the presence of an entrapped, immiscible phase.

2. Methods

[4] We conducted two solute transport experiments in a 15.3 × 30.5 cm, variable-aperture, transparent, analog fracture. In both experiments, we used light transmission techniques to measure the fracture aperture field [*Detwiler et al.*, 1999], the spatial distribution of the entrapped air [*Nicholl et al.*, 2000] and solute concentration fields [*Detwiler et al.*, 2000]. The mean fracture aperture, $\hat{b}$, was 0.0221 cm and the aperture field was stationary with a correlation length, λ, of 0.7 cm. Air injected into the saturated fracture provided a relatively uniform distribution of entrapped air (Plate 1), with water saturation, S_w, of 0.78 and water-occupied mean aperture, $\hat{b}_w$, of 0.0214 cm.

[5] The transport experiments were initiated using the procedure described in detail by *Detwiler et al.* [2000] for saturated solute-transport experiments in the same fracture. A balance recorded outflow for the two experiments yielding measured flow rates (Q) of 0.042 and 0.015 cm^3/s. During each experiment, multiple images (acquired using a charge-coupled-device camera) provided accurate measurements of solute concentration (±2.5% of the injected concentration of Warner Jenkinson, FD&C Blue #1 dye) at high spatial resolution (0.0154 × 0.0154 cm pixels) over the entire flow field. Plates 1a–1c show concentration fields from the Q = 0.042 cm^3/s experiment at t = 0, 34.2, and 68.4 seconds. Note that a data acquisition error caused termination of the Q = 0.015 cm^3/s experiment at t = 160 seconds (prior to the plume reaching the outflow).

[6] We simulated solute transport in the measured aperture field and entrapped-air geometry using a previously developed computational model of solute transport in variable aperture fractures [*Detwiler et al.*, 2000]. This model, which is similar to those used to simulate colloidal transport in variable aperture fractures [*Grindrod and Lee*, 1997; *James and Chrysikopoulous*, 2000], is based on the flow solution from the two-dimensional Reynolds equation

$$\vec{\nabla} \cdot \left(T \vec{\nabla} h \right) = 0; , \tag{1}$$

where $T = b^3 g/(12\nu)$, b is the local fracture aperture, g is the gravitational constant, ν is the kinematic viscosity of the flowing fluid, h is the local head, and local fluxes are given by $\vec{q} = -T\vec{\nabla}h$. The fundamental modification to the saturated solute transport model [*Detwiler et al.*, 2000] is the specification of no-flux boundaries along each air-water interface. This boundary condition is based on the assumption that solute molecules do not adsorb onto air-water interfaces. The excellent mass conservation indicated by our experimental concentration fields confirm that this boundary condition is valid for the solute used in our study.

[7] Solute transport is simulated by tracking particles through a three-dimensional velocity field created by imposing a parabolic velocity profile across the fracture aperture that maintains the local mean velocities predicted by the Reynolds equation. In each time step, particles experience an in-plane advective displacement and a three-dimensional random diffusive displacement; during the advective displacement, a particle moving between grid-blocks with different apertures maintains its relative position between the fracture walls, and particles are reflected at all no-flux boundaries

[1]Now at Division of Geophysics and Global Security, Lawrence Livermore National Laboratory, Livermore, CA, USA.

0094-8276/02/2001GL013508$05.00

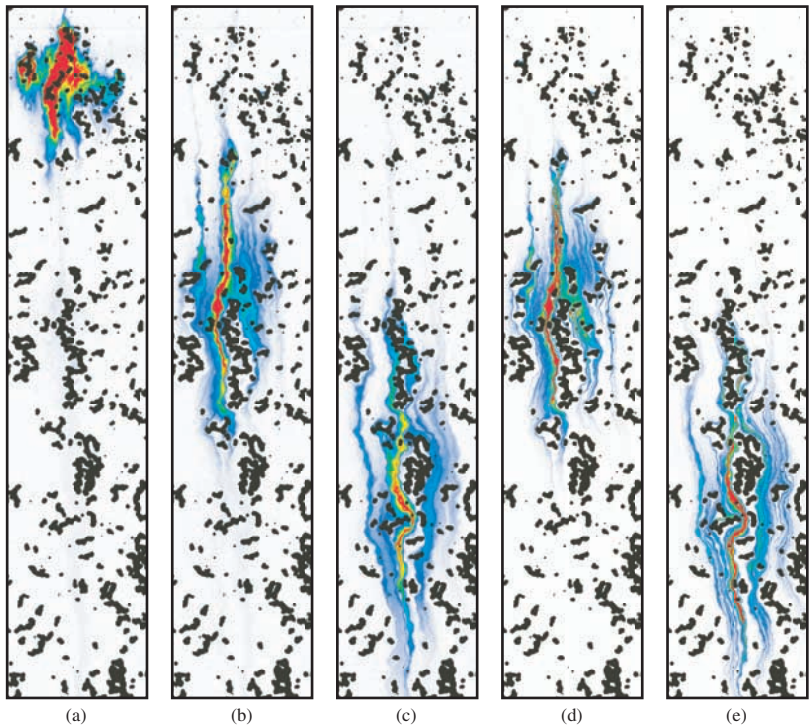

Plate 1. A 6 × 24 cm portion of the initial concentration field for Q = 0.042 cm^3/s at $t = 0$ (a), and the experimental (b, c) and simulated (d, e) concentration fields at t = 34.2 and 68.4 seconds, respectively. The color-scale (white-blue-yellow-red) represents concentrations ranging from 0–0.1 g/l, and black is entrapped air.

(i.e., fracture walls, air-water interfaces, and domain boundaries). For each particle displacement, local values of $\vec{q}$ are calculated by linearly interpolating between the two nearest values. The model uses adaptive time-stepping such that for each particle displacement the advective displacement is less than $\frac{1}{2}$ of the grid spacing and the mean diffusive displacement is less than $\frac{1}{20}$ of the local aperture.

3. Results

[8] The experimental concentration fields (Plates 1a, 1b, and 1c) demonstrate flow channeling induced by the regions of entrapped air within the fracture and diffusion in and out of slow flowing areas near regions of entrapped air, both of which lead to enhanced dispersion. To compare the experiments to simulations, we simulated flow through the measured aperture field (using grid-spacing that corresponded to the aperture measurements) and scaled the resulting head field by a constant to yield a simulated flow rate that matched the measured flow rate. Plates 1d and 1e show the two simulated concentration fields corresponding to the measured concentration fields shown in Plates 1b and 1c and demonstrate good qualitative agreement between the simulation and experiment. The simulation reproduces the channeling around entrapped-air regions observed in the experiment, however, there is slightly less transverse dispersion into low flow areas near the entrapped air. This is likely a result of the inability of the Reynolds equation to accurately describe the true three-dimensional structure of the velocity field, especially near air-water interfaces due to interface curvature, which is not represented in the two-dimensional model.

[9] The first (μ) and second (σ^2) spatial moments of solute mass within the fracture provide additional quantitative measures of solute movement through the fracture. For both experiments and simulations, μ increased linearly with time, which indicates that, despite increased in-plane velocity variations caused by the entrapped air, the mean solute velocity is constant over the duration of the experiments. The simulated first moments are also in close agreement with the experimental results. Fitting a straight line to these plots results in measurements of $\hat{V} = 0.18$ and 0.06 cm/s; based on these velocities and $\hat{b}_w$, Pe = 676 and 230 for the two experiments.

[10] Unlike the results in the saturated fracture [*Detwiler et al.*, 2000], the growth of σ^2 is not linear with respect to time (Figure 1), which indicates that we cannot estimate a single D_L at the scale of these experiments. The shape of the plots of σ^2 versus time are predicted well by the simulations, however, the magnitudes of σ^2 are always underestimated. These results are consistent with the results of experiments and simulations in the saturated fracture

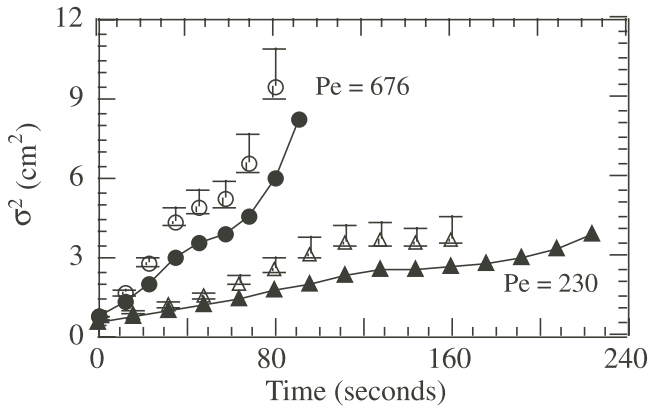

Figure 1. σ^2 plotted against time for the experiments (hollow symbols) and simulations (solid symbols and lines). The error bars represent the results of a sensitivity analysis of the experimental measurements based on the procedure described by *Detwiler et al.* [2000].

[*Detwiler et al.*, 2000], where the inability of the Reynolds equation to fully describe the three-dimensional velocity field was presumed to result in less dispersion. We can quantify the reliability of the model by plotting simulated σ^2 against measured σ^2 (not shown). Fitting straight lines to these plots yields slopes of 0.625 for Pe = 230 and 676, with R^2 = 0.98 and 0.99, respectively, which suggests that the model predicts 62.5% of the experimentally measured dispersion. Because the accuracy of our model is related to the validity of the Reynolds equation, the model will provide better predictions of σ^2 growth in fractures where $\hat{b}/\lambda$ is much smaller than in our experimental fracture.

[11] To evaluate if the simulations in the partially-saturated fracture predict the relative increase in σ^2 caused by the entrapped phase, we plot simulated and measured σ^2 in the saturated fracture against simulated and measured σ^2 (at the same displacements) in the partially-saturated fracture (Figure 2). Fitting straight lines to the data in Figure 2 for experiments 1 and 2, yields slopes that are 17% and 16% larger for the simulations, respectively. This suggests that, for the entrapped phase geometry of these experiments, the model predicts about 84% of the relative increase in dispersion over that simulated in the saturated fracture. Also, the slopes of the lines in Figure 2 demonstrate that, over the scale of these experiments, the additional variability in the velocity field caused by the entrapped phase results in increased dispersion by factors of 3.2 and 2.4 for Pe = 230 and 676, respectively.

[12] Under saturated conditions, D_L exhibited a nonlinear Pe-dependence [*Detwiler et al.*, 2000], highlighting the importance of incorporating out-of-plane velocity variations in transport simulations, particularly for large values of Pe. Though we cannot derive a scale-independent estimate of D_L for the partially-saturated fracture, we can investigate the nature of the Pe-dependence of second moment growth by plotting the second spatial moment against the centroid displacement. If the second moment growth scales linearly with Pe, the plume should have the same second moment at a given displacement, regardless of the time required for that displacement. In Figure 3, the data for experimental and simulated data for Pe = 230 and 676 do not coincide demonstrating nonlinear Pe-dependence of second moment growth (for both the experiments and simulations) due to the velocity profile across the aperture. To illustrate this further, we repeated the simulations with a uniform velocity profile across the aperture, resulting in a linear Pe-dependence of second moment growth and less dispersion than with the parabolic velocity profile (Figure 3). Thus, as in saturated fractures, out-of-plane velocity variations need to be incorporated to consistently predict the nonlinear Pe-dependence of dispersion in partially-saturated fractures.

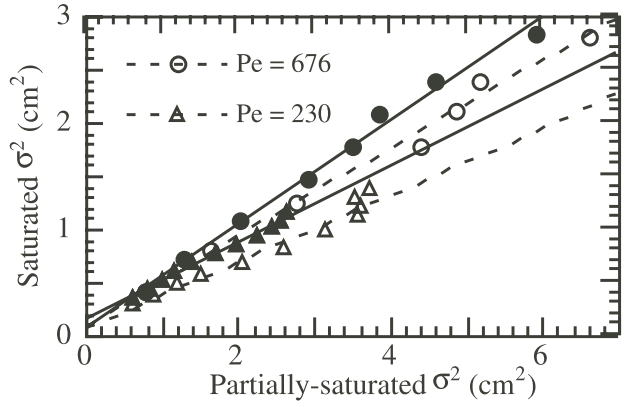

Figure 2. σ^2 in the saturated fracture plotted against σ^2 in the partially-saturated fracture for experiments (hollow symbols) and simulations (solid symbols). The lines (dashed-experiments and solid-simulations) represent a least-squares fit to each set of data.

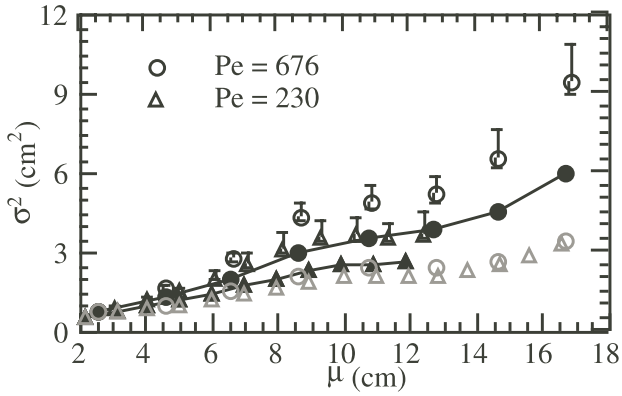

Figure 3. σ^2 plotted against μ for the experiments (hollow black symbols), simulations (solid symbols with lines), and simulations with a uniform velocity profile across the fracture aperture (hollow gray symbols).

4. Concluding Remarks

[13] We have found that a quasi-three-dimensional solute transport model, that incorporates velocity variations in the plane of the fracture (caused by aperture variability and entrapped phase geometry) and across the aperture (modeled using a local parabolic profile), provides good qualitative agreement with experiments in a partially saturated fracture. Though the model consistently underestimates the magnitude of second spatial moments, it predicts all but 16% of the relative increase in solute dispersion resulting from the entrapped phase. The model also correctly predicts a nonlinear Pe-dependence of second moment growth, as observed in the experiments.

[14] For the experiments presented here, the growth of σ^2 with μ was nonlinear, suggesting that D_L had not reached a scale-independent value within the length of the fracture. It is interesting to note that under saturated conditions D_L reached a constant value within a plume displacement of 1.4 cm (about 20 correlation lengths). For D_L to reach a steady value under partially saturated conditions, the plume displacement must be many times the length of the largest entrapped regions in the fracture. Experiments [*Nicholl et al.*, 2000] and simulations [*Glass et al.*, 2001] representing a range of invasion processes, exhibit entrapped regions with a broad range of sizes, even in stationary aperture fields and relatively low entrapped phase saturations. The computational model evaluated here can be used, in conjunction with phase invasion models, to investigate the influence of the entrapped phase on solute transport in partially-saturated fractures. These studies will further clarify the role of entrapped-phase geometry on the scale-dependence of dispersion in partially-saturated fractures and motivate approaches for quantifying the deviations from Fickian behavior.

[15] **Acknowledgments.** This work was supported by the U.S. Department of Energy's Basic Energy Sciences Geoscience Research Program under contract numbers DE-FG03-96ER14590 (University of Colorado) and DE-AC04-94AL85000 (Sandia National Laboratories). Experiments were conducted at the Flow Visualization and Processes Laboratory at Sandia National Laboratories. We thank the anonymous reviewers for their helpful comments.

References

Detwiler, R. L., S. E. Pringle, and R. J. Glass, Measurement of fracture aperture fields using transmitted light: An evaluation of measurement

errors and their influence on simulations of flow and transport through a single fracture, *Water Resour. Res.*, *35*, 2605–2617, 1999.

Detwiler, R. L., H. Rajaram, and R. J. Glass, Solute transport in variable-aperture fractures: An investigation of the relative importance of Taylor dispersion and macrodispersion, *Water Resour. Res.*, *36*, 1611–1625, 2000.

Glass, R. J., M. J. Nicholl, and V. C. Tidwell, Challenging models for flow in unsaturated, fractured rock through exploration of small scale flow processes, *Geophys. Res. Lett.*, *22*, 1457–1460, 1995.

Glass, R. J., and M. J. Nicholl, Quantitative visualization of entrapped phase dissolution within a horizontal flowing fracture, *Geophys. Res. Lett.*, *22*, 1413–1416, 1995.

Glass, R. J., H. Rajaram, M. J. Nicholl, and R. L. Detwiler, The interaction of two fluid phases in fractured media, *Current Opinion in Colloid & Interface Science*, *6*(3), 223–235, 2001.

Grindrod, P., and A. J. Lee, Colloid migration in symmetrical non-uniform fractures: Particle tracking in three dimensions, *J. Contam. Hydrol.*, *27*, 157–175, 1997.

Ippolito, I., G. Daccord, E. J. Hinch, and J. P. Hulin, Echo tracer dispersion in model fractures with a rectangular geometry, *J. Contam. Hydrol.*, *16*, 87–108, 1994.

James, S. C., and C. V. Chrysikopoulous, Transport of polydisperse colloids in a saturated fracture with spatially variable aperture, *Water Resour. Res.*, *36*, 1457–1465, 2000.

Nicholl, M. J., H. Rajaram, and R. J. Glass, Factors controlling satiated relative permeability in a partially-saturated horizontal fracture, *Geophys. Res. Lett.*, *27*, 393–396, 2000.

Roux, S., F. Plouraboue, and J. P. Hulin, Tracer dispersion in rough open cracks, *Trans. Porous Media*, *32*, 97–116, 1998.

R. L. Detwiler, Lawrence Livermore National Laboratory, P.O. Box 808, L-206, Livermore, CA 94551, USA. (detwiler1@llnl.gov)

H. Rajaram, Department of Civil, Environmental, and Architectural Engineering, 428 UCB, University of Colorado, Boulder, CO 80027, USA. (hari@colorado.edu)

R. J. Glass, Flow Visualization and Processes Laboratory, Sandia National Laboratories, Albuquerque, NM 87185-1345, USA. (rjglass@sandia.gov)